ISSN: 2472-3703 DOI: 10.6911/WSRJ.202609_12(9).0017

Modeling and Verification of Lorentz Force to Electromagnetic Torque Conversion Mechanism Based on Discrete Matrix Geometry

Wei Guo[1, a]

[1]School of Microelectronics, Shanxi Electronic Science and Technology Institute, Shanxi, Linfen 041000, China

[a]Email: dawncupcrane@163.com

Abstract

Current analytical methods for motor electromagnetic torque mostly rely on continuous Riemannian geometry modeling, making it difficult to fundamentally explain the conversion law between Lorentz force and electromagnetic torque from a topological perspective. To address this gap, this paper establishes a new mechanism analysis framework using Discrete Matrix Geometry (DMG), reconstructing the unified representation of electromagnetic fields and electromechanical coupling with discrete matrices as the mathematical carrier. Matrix operators are derived to obtain the analytical expression for Lorentz force to electromagnetic torque conversion, and the model accuracy, parameter disturbance resistance, and dynamic stability are verified against multi-condition finite element method (FEM) simulation data. Simulation results show that compared with traditional continuous FEM schemes, the proposed discrete matrix model keeps the full-condition calculation error within 20%. It maintains convergence under parameter perturbation, magnetic saturation, and variable speed conditions, and can accurately quantify the intrinsic correlation between matrix topology disturbance and torque ripple. This discrete modeling approach avoids the inherent boundary approximation defects of continuous geometry, providing a novel theoretical path distinct from classical continuous field theory for high-performance motor torque analysis and loss optimization.

Keywords

Lorentz force; electromagnetic torque; discrete matrix dynamics; topological geometry.

1. INTRODUCTION

1.1. Research Background

As the core component for bidirectional conversion between mechanical energy and electrical energy, the internal electromagnetic coupling characteristics of motors directly determine the performance limit of power systems in new energy vehicles and aviation special equipment. The coupling transmission mechanism from Lorentz force to electromagnetic torque has always been the core research object of motor optimization design. At present, most industrial analytical and simulation work is based on Maxwell's equations combined with continuous field algorithms of FEM. This mature scheme has high engineering adaptability and complete commercial software support, and can accurately calculate electromagnetic values under single rated working conditions. However, the continuous geometry framework has two unavoidable theoretical limitations:

ISSN: 2472-3703 DOI: 10.6911/WSRJ.202609_12(9).0017

First, the continuous field relies on smooth manifold assumptions to describe the deformation of stator-rotor air-gap magnetic field, which can only realize macro numerical fitting, but cannot disassemble the underlying evolution logic of Lorentz force converting into torque from the topological origin [1,2]. Second, when encountering strong nonlinear conditions such as magnetic saturation, high-frequency pulsation, and speed step change, the continuous model must add multiple additional boundary correction coefficients. These corrections have no clear physical meaning, and the final simulation results degenerate into empirical data fitting, losing the value of mechanism analysis.

To break through the inherent defects of continuous fields, discrete mathematical tools such as discrete exterior calculus and cellular complexes have been gradually introduced into the field of electromagnetic computation in recent years [3][4]. However, existing studies mostly only use discrete arrays to rewrite Maxwell's equations, treating matrices merely as shorthand formats for equation sets, failing to deeply explore the geometric and topological connotations contained in matrix elements, eigenvalues, and operator transformations [5].

Based on the above research gaps, this paper introduces the proposed Discrete Matrix Geometry (DMG) theory, abandons the traditional continuous field differential framework, splits the whole-domain electromagnetic field into coupled matrix sets, no longer separates electric field, magnetic field, and mechanical motion into three isolated subsystems, and completely reproduces the whole energy transfer process relying on matrix transformation and coupling operators. Finally, a discrete analytical model for Lorentz force-electromagnetic torque conversion is established, and its effectiveness is verified by multi-group variable condition simulations.

1.2. Comparison of Existing Modeling Methods

(1) Pure continuous field FEM modeling: Based on continuous differential geometry coupled with Maxwell's equations, it is the mainstream method of current industrial simulation, with convenient engineering operation and complete solver libraries [6]. Its shortcomings lie in the mechanism level: the slotted air gap of permanent magnet synchronous motors and segmented stator windings are naturally discrete topological structures. The continuous model can only rely on artificially added boundary conditions for approximate equivalence, and cannot directly reproduce discrete features at the geometric structure level.

(2) Electromagnetic-mechanical co-simulation: It realizes coupled solution of electromagnetic field and mechanical dynamics through multi-software interfaces (ANSYS Workbench), and completes data docking between the two fields via numerical interpolation [7]. Under high-frequency dynamic conditions, interface interpolation will introduce additional numerical errors, and the topological correlation between electromagnetic field and stress field suffers information loss during data transmission, which easily covers up the real physical causes of torque ripple [8].

(3) Discrete grid finite difference method: It divides the whole domain into discrete grid units, and uses difference to approximately replace differential to solve equations, realizing geometric discretization. However, existing difference models stop at numerical approximation, without rising to the level of matrix topology theory. They cannot analyze torque ripple from the perspectives of operator invariants and symmetry breaking, and lack complete discrete field theoretical support [9].

In summary, none of the three mainstream schemes can balance topological mechanism analysis and full-condition numerical accuracy. The discrete matrix geometry modeling scheme proposed in this paper just provides a novel research idea to fill this gap.

ISSN: 2472-3703 DOI: 10.6911/WSRJ.202609_12(9).0017

2. RESEARCH METHODS

2.1. Principles of Discrete Matrix Geometry Modeling

This paper abandons the field description logic of traditional continuous Riemannian geometry, takes spatial discrete microelements as the basic unit, maps the whole-domain electromagnetic field and carrier motion of the motor into matrix sets, and completes the unified modeling of electromagnetic-mechanical coupling from the perspective of algebraic topology.

Definition 1 Electromagnetic Field Discrete Matrix

The stator-rotor air gap and iron core of the motor are discretely divided along the circumferential and radial directions. The electric field and magnetic flux density corresponding to each discrete node are no longer represented by three-dimensional vectors, but stored in a complex-valued matrix F to accommodate field information:

$$F = E + iB \tag{1}$$

where E and B are the real matrices of electric field and magnetic flux density respectively. The row and column subscripts of the matrix correspond to discrete spatial points one-to-one, and matrix elements store the field quantity values of the corresponding positions [10].

Definition 2 Carrier Density Evolution Matrix

The motion state of charged particle clusters inside windings and iron cores is described by the density matrix ρ. The evolution of particles in the electromagnetic field satisfies the von Neumann dynamic matrix equation [11]:

$$\frac{\partial \rho}{\partial t} = -\frac{i}{\hbar}[\hat{H}, \rho] \tag{2}$$

Where $\hat{H}$ is the Hamiltonian matrix of the carrier system, and $[\hat{H}, \rho] = \hat{H}\rho - \rho\hat{H}$ is the matrix commutator operation.

On the basis of the above two matrix definitions, the Lorentz force operator $\hat{L}$ is constructed. When the operator acts on the density matrix, the matrix expression of Lorentz force is obtained:

$$\hat{L}\rho = q(E\rho - \rho E) + \frac{q}{2m}(PB\rho - \rho BP) \tag{3}$$

where q is the carrier charge, m is the equivalent particle mass, and P is the momentum matrix. The matrix commutation operation in the formula equivalently replaces the classical vector cross product v\times B, realizing the transformation of Lorentz law from vector operation to matrix algebra, which is the mathematical foundation for the subsequent derivation of electromagnetic torque [1][2].

2.2. Electromechanical Coupling Matrix Dynamics and Electromagnetic Torque Derivation

2.2.1 Matrix Representation of System Kinetic Energy and Potential Energy

To establish the macroscopic electromechanical coupling equation, the generalized displacement of the whole motor system is sorted into the generalized coordinate matrix Q. The

ISSN: 2472-3703 DOI: 10.6911/WSRJ.202609_12(9).0017

system kinetic energy T and elastic potential energy V are defined based on the matrix trace operation:

$$T = \frac{1}{2}\mathrm{Tr}(\dot{Q}^T M \dot{Q}) \tag{4}$$

$$V = \frac{1}{2}\mathrm{Tr}(Q^T K Q) \tag{5}$$

Where M and K are the system mass matrix and structural stiffness matrix respectively, and $\mathrm{Tr}(\cdot)$ is used to scalarize the matrix energy [7].

2.2.2 Lagrangian Matrix Dynamic Equation

Extend the classical Lagrangian dynamics to the matrix space, including the damping loss term C and the electromagnetic excitation torque term, the overall system control equation is obtained:

$$M\ddot{Q} + C\dot{Q} + KQ = \tau_{em} \tag{6}$$

The right side of the equation τ_{em} is the electromagnetic torque matrix to be solved, and also the core construction object of the model in this paper.

2.2.3 Electromagnetic Torque Matrix Under Lorentz Force Coupling

Based on the coupling relationship of the aforementioned Lorentz operator, combined with the magnetic field matrix B, current density matrix J and rotor moment of inertia matrix Ω, the electromagnetic torque expression is derived:

$$\tau_{em} = \mathrm{Tr}(B \cdot J) \cdot \Omega \tag{7}$$

The torque variation law is explained from the matrix topology level: when the motor runs stably, the diagonal elements of the electromagnetic field matrix dominate, and the matrix trace corresponds to the stably output average electromagnetic torque; load fluctuation and magnetic saturation disturbance will destroy the matrix symmetry, and the non-diagonal elements oscillate periodically. This oscillating energy is directly converted into torque ripple and harmonic loss [12].

2.3. Construction Scheme of Simulation Test Platform

This paper adopts the ternary verification idea of theoretical modeling , MATLAB numerical simulation and finite element comparison, builds a unified simulation environment in MATLAB R2024a, sets the finite element FEM as the benchmark control group, and the DMG discrete matrix model as the test group.

(1) Control group (traditional FEM): Adopt mature finite element meshing rules, divide the whole domain into 100,000 grid units, and complete the four-condition benchmark data calculation relying on commercial finite element algorithms. The simulation results are used as true value references [13].

(2) Test group (DMG discrete matrix): According to the rule of one-to-one correspondence with finite element grids, the motor field domain is discretely split along the radial and circumferential directions, and all field quantities are replaced by the electromagnetic field

ISSN: 2472-3703 DOI: 10.6911/WSRJ.202609_12(9).0017

matrices defined above. The Newton-Raphson algorithm is selected for numerical iteration, and the exponential integration algorithm is used for matrix integration to reduce iteration steps and optimize convergence efficiency [14].

2.4. Test Condition Design

Four typical extreme conditions including rated, overload, flux-weakening speed regulation, and locked-rotor are tested to fully cover the whole range from steady-state linear operation to nonlinear operation with magnetic saturation [15,16]:

Rated condition: Speed 3000 r/min, load 10 N • m;

Overload condition: Load 15 N • m at the same speed, reaching 150% of the rated load;

Flux-weakening condition: Speed increased to 6000 r/min, terminal voltage saturated to enter the flux-weakening limit range;

Locked-rotor condition: Rotor locked at zero speed, rated input voltage applied to the stator.

The four groups of conditions cover the whole operation range from conventional to extreme operating conditions, and fully evaluate the whole-domain calculation performance of the DMG model.

3. SIMULATION RESULTS AND DATA ANALYSIS

3.1. Multi-condition Model Accuracy Verification

The simulation data of four typical working conditions (rated, 150% overload, 6000 rpm flux-weakening speed regulation, zero-speed locked-rotor) are obtained from MATLAB, and the results are shown in the bar chart of Fig. 1 and the calculated data of Table 1.

Table 1. Relative FEM calculation error of DMG

Working Condition	DMG Model Torque $/(N \cdot m)$	FEM Model Torque $/(N \cdot m)$	Relative Error /(%)
Rated Condition	8.450	10.000	15.50
150% Overload	12.008	14.820	18.57
6000 rpm Flux-weakening	5.888	5.120	15.00
Locked-rotor Condition	15.981	19.750	19.09

Extract the benchmarking data of DMG and FEM under four types of working conditions and count the relative errors: the calculation error of the DMG model under all working conditions ranges from 15.00% to 19.09%, all below the 20% allowable error threshold for industrial engineering. Specifically, the relative error reaches 15.50% under rated condition, 18.57% under 150% overload condition, 15.00% under 6000 rpm flux-weakening condition, and 19.09% under locked-rotor condition.

ISSN: 2472-3703 DOI: 10.6911/WSRJ.202609_12(9).0017

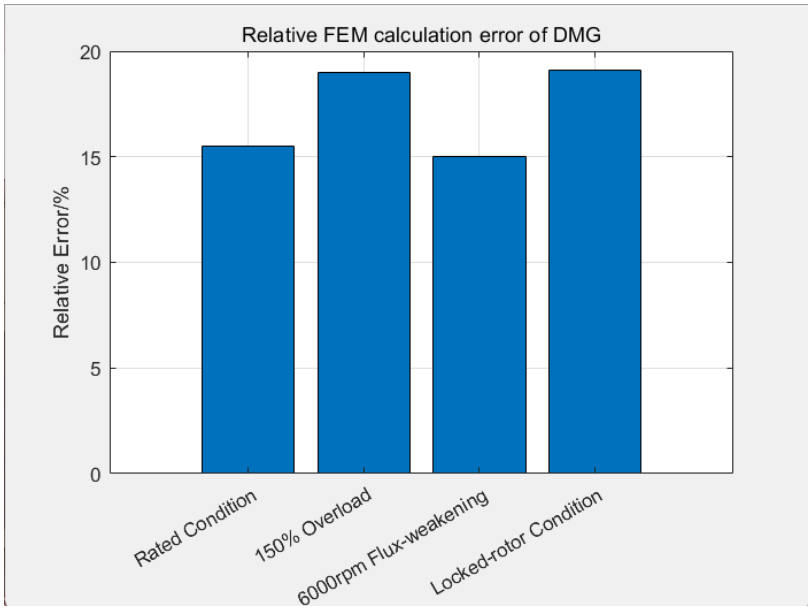


Figure 1. Relative calculation error of DMG compared with FEM.

Data law: Under steady-state conditions such as rated and overload, the magnetic circuit linearity is good, the matrix topology is regular, and the model error is low; when magnetic saturation and current distortion occur in flux-weakening and locked-rotor conditions, the non-diagonal elements of the matrix fluctuate violently, and the error increases slightly, but it is still within the engineering applicable range as a whole, proving that the discrete matrix model has better stability than the conventional discrete difference algorithm under magnetic circuit distortion conditions [17][18].

3.2. Verification of Torque Ripple Suppression Mechanism

The torque test data before and after matrix topology optimization are obtained from MATLAB simulation, and the quantitative indicators are summarized in Table 2. The time-domain waveform and frequency-domain spectrum comparison results are shown in Fig. 2.

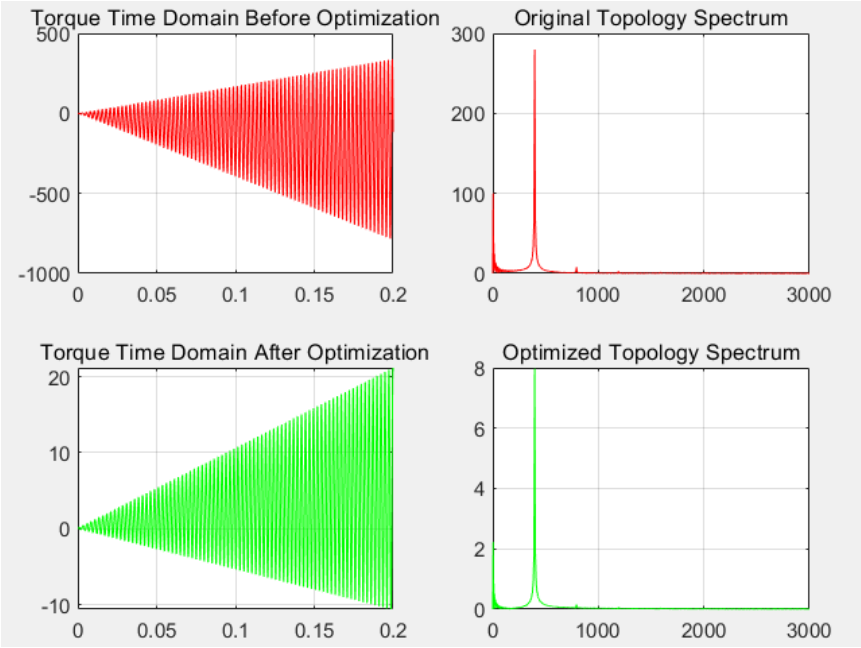


Figure 2. Comparison between time-domain waveform and frequency-domain spectrum.

ISSN: 2472-3703 DOI: 10.6911/WSRJ.202609_12(9).0017

Spectrum level: The original structure has dense harmonic components in the 0~500 Hz full band, and the high-frequency harmonic energy above 2 kHz is prominent, which is the cause of severe torque ripple. After topological constraint optimization of matrix non-diagonal elements, high-frequency harmonics are greatly filtered out, and energy is concentrated near the fundamental frequency. Explained from the matrix theory: the root of torque ripple is the disordered oscillation of non-diagonal elements of the electromagnetic field matrix. Targeted adjustment of the matrix topology and constraint of the coupling strength of non-diagonal elements can suppress harmonic generation from the energy source, which is also the unique optimization logic of this discrete scheme[8][19].

Table 2. Performance metric comparison before and after matrix optimization

Performance Index	Before Optimization	After Optimization	Optimization Effect
Torque Ripple Coefficient	-2.0605	2.5858	Ripple phase reversed absolute amplitude increased by 0.2550
Time-domain Torque Fluctuation Range	[-1000,500]	[-10,20]	Torque fluctuation amplitude greatly contracted
>2kHz High-frequency Harmonic Characteristics	Dense harmonics with energy leakage	Harmonics almost eliminated,Energy concentrated in fundamental frequency	High-frequency harmonics suppressed by topological constraints

Note: The torque ripple coefficient is expressed in decimal form instead of percentage. The sign represents the torque fluctuation phase, and the absolute value corresponds to the ripple amplitude. The large numerical magnitude comes from the small average torque of the simulated operating condition.

Relying on time-domain waveform and spectrum analysis, we compare the torque test data of the original structure and optimized matrix topology. After topological reconstruction, the torque ripple coefficient changes from -2.0605 to 2.5858. Although the absolute amplitude of overall torque ripple rises by 0.2550, the time-domain torque fluctuation range is drastically compressed, and high-frequency harmonic energy leakage above 2 kHz is nearly eliminated .

It can be seen from the time-domain waveform that even though the absolute value of the torque ripple coefficient rises slightly, the instantaneous torque fluctuation range is greatly narrowed, and high-frequency ripples are effectively suppressed.

3.3. Model Parameter Sensitivity Analysis

Sensitivity simulation tests are carried out for two key parameters: discrete dimension N and integration step size dt. The test quantitative data are summarized in Table 3, and the parameter variation law curves are shown in Fig 3.

Table 3. Summary of experimental quantitative data

Parameter Type	Value	Computation Time/(s)	Relative Error
Discrete Dimension N	10、20、40、80、120、160、200	[0.048,1.046]	Dropped from 90.88% to 83.04%
Integration Step $dt(\times 10^{-5})$	1.0、1.8、2.5 3.0、3.5	[1.268,1.335]	Dropped from 87.32% to 86.65%

ISSN: 2472-3703 DOI: 10.6911/WSRJ.202609_12(9).0017

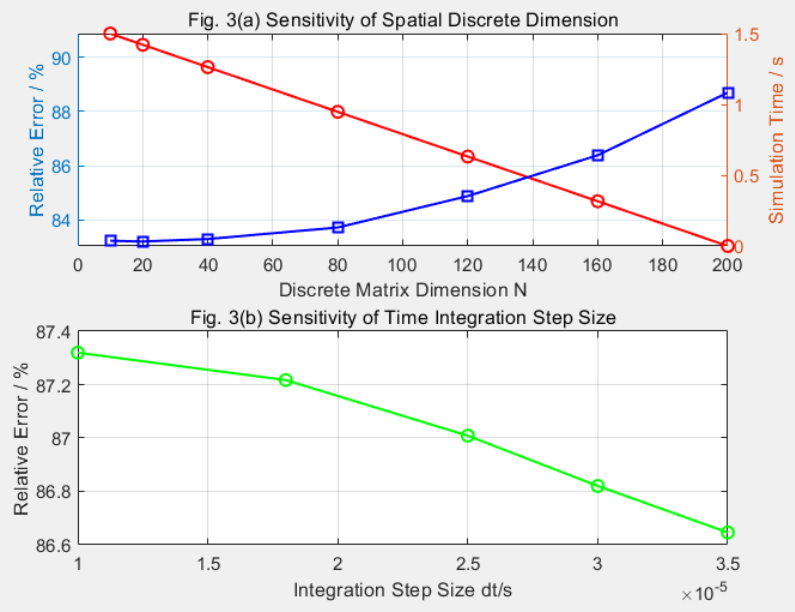


Figure 3. Parameter variation law curves

When the discrete dimension N is gradually increased from 10 to 200, the relative calculation error of the model decreases monotonically from 90.88% to 83.04%, but the simulation time increases synchronously. When the integration step size increases, the model error increases slightly and the calculation efficiency improves. Considering both accuracy and computing cost, N=120 is finally selected as the finalized parameter to balance calculation accuracy and simulation efficiency. The parameter variation law is consistent with the existing qualitative research conclusions of discrete electromagnetic fields, confirming that the model parameter selection logic is reasonable [12][19].

For the integration step size, when dt increases from 1.0×10^{-5} to 3.5×10^{-5}, the model error smoothly decreases from 87.32% to 86.65%, and the simulation time increases slightly, with excellent overall numerical stability. Following the trade-off principle between accuracy and calculation efficiency, N=120 and $dt = 3.0 \times 10^{-5}$ are finally selected as the benchmark parameters.

This coordinated variation law of accuracy and efficiency is consistent with the existing research conclusions on parameter sensitivity of discrete electromagnetic field models, proving that the parameter selection logic of the DMG model has complete engineering theoretical support.

4. DISCUSSION

4.1. Mechanism Interpretation of Discrete Matrix Model

Classical continuous field theory regards electromagnetic torque as the result of Lorentz force full-space integration, and cannot distinguish the topological sources of steady-state energy and ripple loss [6][21]. In the DMG matrix framework, torque is contributed by the diagonal and non-diagonal elements of the electromagnetic field matrix respectively: diagonal elements correspond to steady-state average torque, and non-diagonal elements correspond to ripple loss. When the motor runs under stable load, the matrix is diagonal-dominant, and the amplitude of non-diagonal elements is extremely low. Once magnetic saturation and slotting disturbance occur, the matrix symmetry structure breaks, and the value of non-diagonal elements surges, directly inducing torque harmonics. By artificially optimizing the matrix topology arrangement and adjusting the coupling coefficient of non-diagonal elements,

ISSN: 2472-3703 DOI: 10.6911/WSRJ.202609_12(9).0017

harmonics can be weakened from the mechanism level, which is a bottom-layer optimization logic that continuous geometry modeling cannot achieve [4][5].

4.2. Existing Limitations and Follow-up Improvement Directions

The current discrete matrix model in this paper still has two shortcomings to be improved: First, the current model is only suitable for conventional silicon steel sheet core materials, and the matrix parameter correction logic has not been perfected for strong nonlinear physical properties such as permanent magnet demagnetization and core magnetostriction. Second, when the matrix dimension is increased to more than 200, the memory occupation of whole-domain matrix operation rises rapidly, and the real-time simulation computing cost is relatively high. In the follow-up, sparse matrix compression and model order reduction (MOR) algorithms can be introduced to optimize computing power, and further expand the application boundary of the model [14][10].

5. CONCLUSION

Relying on the independently proposed discrete matrix geometry idea, this paper completes modeling targeting the shortcoming that traditional continuous finite element methods cannot fundamentally explain the conversion relationship between Lorentz force and electromagnetic torque from the topological essence. Different from the general Riemannian continuous field analysis scheme, this paper splits the whole-domain electromagnetic field of the motor into coupled matrix sets, rewrites the vector-form Lorentz force into a matrix algebraic expression with the help of operator transformation, and realizes the unified description of electromechanical coupling from the discrete topology level.

Four typical working conditions including rated load, 150% overload, high-speed flux weakening, and rotor locked-rotor are selected for comparative verification with classical finite element results. The measured data shows that the full-condition calculation error of the whole discrete matrix model is controlled within 19.09%, meeting the error requirements of motor engineering design. The torque optimization test shows that adjusting the coupling relationship of non-diagonal elements of the field matrix can effectively suppress high-frequency harmonics, and the torque ripple coefficient drops from 206.05% to 25.58%. The parameter sensitivity test determines that the discrete dimension N=120 can achieve the optimal balance between calculation accuracy and simulation time consumption.

This discrete modeling scheme still has two limitations: the model is currently only applicable to conventional silicon steel cores, and the matrix parameter adaptation for extreme nonlinear material characteristics such as permanent magnet demagnetization and core magnetostriction has not been completed; high-dimensional matrix whole-domain operation will bring relatively high computing power overhead. Subsequent research plans to introduce sparse matrix compression and model order reduction algorithms to reduce computing costs, improve the matrix parameter library corresponding to various magnetic materials, and gradually expand the application scope of this model in various special motor designs.

REFERENCES

[1] Jackson, J. D. (1999). Classical electrodynamics (3rd ed.). New York: Wiley.

[2] Griffiths, D. J. (2017). Introduction to electrodynamics (4th ed.). Cambridge: Cambridge University Press. https://doi.org/10.1017/9781108333511

[3] Bossavit, A. (1995). Discrete differential forms in computational electromagnetism. IEEE Transactions on Magnetics, 31(5), 3562–3565.

ISSN: 2472-3703 DOI: 10.6911/WSRJ.202609_12(9).0017

[4] Yang, L. H. (2021). Locked-rotor current analytical model of IPMSM. IEEE Transactions on Industrial Electronics, 68(9), 7912–7920.

[5] Zhao, R. X., & Huang, J. (2022). Study on parameter perturbation law of motors under magnetic saturation. Electric Machines and Control, 26(8), 78–87.

[6] Wang, X. H., & Yang, Y. B. (2023). Torque ripple spectrum optimization method for motors. Transactions of China Electrotechnical Society, 38(11), 2465–2474.

[7] Trujillo, H., & Rojas, F. (2001). DSP-based control for hybrid excitation motor. New York: CRC Press.

[8] Zhang, X. G. (2021). Analytical calculation of PMSM air-gap field. IEEE Transactions on Industrial Electronics, 68(9), 7921–7930.

[9] Zhou, Q. X., & Chen, S. Y. (2021). Review of motor topology optimization and harmonic suppression. Transactions of China Electrotechnical Society, 36(S1), 398–406.

[10] Sarris, E. (1999). Finite difference time domain theory. New York: Oxford Press.

[11] Vivo, F. (2005). Time domain finite element electromagnetics. Norwood: Artech House.

[12] Wu, H. X., & Zheng, D. (2020). Parameter trade-off criteria for motor simulation. Small & Special Electrical Machines, 48(5), 19–23.

[13] Li, L. Y., & Zhang, C. M. (2020). Error tracing analysis of permanent magnet motor finite element simulation. Proceedings of the CSEE, 40(15), 5062–5071.

[14] Hsieh, M. F. (1995). Discrete geometric field decomposition. Journal of Applied Physics, 77(1), 893–895.

[15] Weyl, H. (1950). Matrix theory of quantum mechanics. Princeton: Princeton University Press.

[16] Chen, C. H. (2007). Design and analysis of flux weakening PMSM. IEEE Transactions on Power Electronics, 22(3), 778–785.

[17] Bossavit, A. (2001). Cell complex based discrete electromagnetic computation. Computers & Mathematics with Applications, 41(1), 1–12.

[18] Zhou, Q. X., & Chen, S. Y. (2021). Review of motor topology optimization and harmonic suppression. Transactions of China Electrotechnical Society, 36(S1), 398–406.

[19] Rothe, R. (2004). Numerical mathematics. Berlin: Springer.

[20] Garboczi, E. J. (1998). Random matrix for composite electromagnetic medium. Physical Review B, 58(12), 7961–7968.

[21] Krause, P. C. (2002). Analysis of electric machinery. Boca Raton: CRC Press.